

SIGN: A Statistically-Informed Gaze Network for Gaze Time Prediction

Jianping Ye Michel Wedel
The University of Maryland
College Park, MD 20742, USA
{jpye00, mwedel}@umd.edu

Abstract

We propose a first version of SIGN, a Statistically-Informed Gaze Network, to predict aggregate gaze times on images. We develop a foundational statistical model for which we derive a deep learning implementation involving CNNs and Visual Transformers, which enables the prediction of overall gaze times. The model enables us to derive from the aggregate gaze times the underlying gaze pattern as a probability map over all regions in the image, where each region’s probability represents the likelihood of being gazed at across all possible scan-paths. We test SIGN’s performance on AdGaze3500, a dataset of images of ads with aggregate gaze times, and on COCO-Search18, a dataset with individual-level fixation patterns collected during search. We demonstrate that SIGN (1) improves gaze duration prediction significantly over state-of-the-art deep learning benchmarks on both datasets, and (2) can deliver plausible gaze patterns that correspond to empirical fixation patterns in COCO-search18. These results suggest that the first version of SIGN holds promise for gaze-time predictions and deserves further development.

1. Introduction

Building human-like visual systems is a fundamental goal in machine learning. The recognition of the central role of human eye movements in visual perception and attention has led to a surge of interest in the development of deep learning models of human gaze. For example [12, 13] show that Convolutional Neural Networks (CNN) can generate human-like scanpaths better than traditional methods, such as [9]. Long Short-Term Memory (LSTM) models [3, 6], inverse reinforcement learning [5], Transformers [18] and Large Language Models [4], have enabled the sequential modeling of gaze patterns by including high-level semantic information to improve visual tasks such as object detection [17, 27], semantic segmentation [15, 29], visual question answering [4], and decision making [2, 25].

For training and inference, these prior models rely on

eye-tracking data comprising of individual-level fixation patterns. Instead, in the present study we develop a computational gaze model that is trained on *aggregate gaze time data*. Aggregate gaze data arise frequently when data collection is constrained by data privacy laws (such as GDPR) or because of the costs, complexity and scalability of data storage and processing pipelines. Research companies collect many hundreds of eye-tracking datasets per year, and oftentimes collect or retain only the aggregated gaze times on commercial images. Aggregate gaze times are of great interest because they reflect the depth of attention and offer insights into cognitive engagement in applications such as advertising and human-computer interaction [22, 30].

Therefore, we develop a machine learning model to predict gaze times, called SIGN (Statistically-Informed Gaze Network). We start with a foundational statistical model that extends prior work (e.g., [16, 23]), which we implement as a deep neural network that enables prediction of aggregate gaze time data. SIGN allows us to derive from the aggregate gaze times the underlying gaze pattern as a probability map over all spatial regions in the image, where each region’s probability represents the likelihood of attracting gaze across all possible scan-paths. We validate our model on two datasets: AdGaze3500 and COCO-Search18; the former contains aggregate gaze times on advertisements, the latter individual-level fixation sequences on images of scenes. The results show that our approach achieves better performance in gaze time prediction than state-of-the-art deep learning methods, while the inferred gaze patterns align well with empirical fixation patterns.

2. Methods

We first propose a foundational statistical scan-path model. Our contribution over prior statistical models [16, 23] is that we relax the first order Markov assumption and include image features. The model describes aggregate gaze times, for which previously mostly linear, hierarchical linear, and tree models have been used [22, 28, 30]. The model assumes scan-paths, trajectories of fixations of the eyes [19], to underlie gaze time on images that appear

within a context (such as images on websites, or ads within magazines).

2.1. Gaze Model Formulation

The foundational model is based on the following assumptions, which are grounded in prior empirical findings.

Assumption 1. Gaze time is *additive* in the log space of time, that is, the log gaze time arises as a sum of a series of log fixation durations on regions of the image.

Assumption 2. The log gaze g for an image is generated by the following stochastic process with the state space $\mathcal{S} = \{S_1, \dots, S_N\}$, consisting of local K -dimensional feature vectors for N regions on image I : let $(F_t)_{t=1}^{\tilde{T}} \in \{1, \dots, N\}^{\tilde{T}}$ be fixations on regions of I , I^c be the context if present, with $\tilde{T} \in \mathbb{Z}^+$ the (predetermined) total number of fixations. For $t \leq \tilde{T}$ the generative process is:

1. During scene exploration the first fixation often lands in the center [24]; within a single fixation the gist of the scene is extracted [21]. Generate F_0 to be the center point of the blurred and down-scaled image \tilde{I} , with features S_0 that capture the ‘‘gist’’. Assuming that the influence of the context operates via its gist, generate the initial fixation duration $g_0 = \mu_0(S_0, S_c)$, with features S_c that capture the gist of the context I^c .
2. According to Inhibition of Return (IoR) [11] visited states are less likely to be visited again. Generate the transition probability \hat{E} from previous fixation F_{t-1} to the next state S_j with $\hat{E}_j = \hat{E}_j((S_{F_{t-k}})_{k=1}^{t-1}, S_j)$, such that $\sum_j \hat{E}_j = 1$ and $\hat{E}_{F_l} = 0$ for all $l = 1, \dots, t$. Sample the next fixation F_t from Categorical(\hat{E}).
3. Fixation durations are affected by image features [20]. Generate log-fixation duration g_t , $t \geq 1$, from some distribution \mathcal{D} with mean $\mu(S_{F_t})$ governed by features at the current fixation on the image, S_{F_t} .

Remarks: (1) Because the length of a scan-path is finite, we assume it is bounded above by \tilde{T} ; (2) The (infinite horizon) IoR can be relaxed to a fixed time horizon.

Assumption 3. If G is the gaze time on the image I with context I^c , then:

$$\mathbb{E}(G) = \exp(\mathbb{E}g),$$

where $g = g_0 + \sum_{t=1}^{\tilde{T}} g_t$ generated from the process in Assumption 2. This assumption allows us to use observed aggregate gaze times to fit the model.

Problem Formulation. Here we formulate our model based on the three assumptions. We divide I into equal spatial regions (image patches) with non-overlapping local features (states) $\{S_1, \dots, S_N\}$. We use μ_0 to represent the initial log-fixation duration on the features S_0 of the blurred image \tilde{I} , and μ to represent the log-fixation duration determined by local features S_j of region j . Since the length of a scan-path is finite, the expected log gaze g is:

$$\mathbb{E}(g) = \mu_0(S_0, S_c) + \sum_{\tau} P_{\tau} \sum_i \mu(S_{\tau_i}), \quad (1)$$

where τ is one scan-path $(F_t)_{t=1}^{\tilde{T}}$, i indicates the regions visited in the scan-path τ , and P_{τ} is the associated probability of τ . Note that P_{τ} is a function of the features $\{S_j\}$, since the transition probabilities are determined by local features of the image by step 2 of assumption 2. Because we assume that we have no access to individual fixation locations, we invoke IoR (Assumption 2) and rearrange the terms, which yields:

$$\mathbb{E}(g) = \mu_0(S_0, S_c) + \sum_{j=1}^N \mu(S_j) w_j, \quad (2)$$

with weights w_j defined by

$$w_j = \sum_{\tau \in \mathcal{T}_{S_j}} P_{\tau}, \quad (3)$$

where \mathcal{T}_{S_j} is the set of all scan-paths that contain region S_j . Let us call the first and the second terms in equation 2 ‘‘gist’’ gaze and total local gaze, respectively. As a result of Assumption 3, equation 2 can be estimated if one replaces the left hand side by the log of the empirical average gaze time. This is important in many practical situations where only the average gaze time data is available.

Inferred Gaze Pattern We define the inferred fixation pattern as:

$$p_{S_j} = \frac{w_j}{\sum_k w_k} = \frac{\sum_{\tau \in \mathcal{T}_{S_j}} P_{\tau}}{\sum_k \sum_{\tau \in \mathcal{T}_{S_k}} P_{\tau}} \quad (4)$$

for $j = 1, \dots, N$. We observe that the weights in equation 3 indicate the frequency with which an individual will fixate on local features S_j : the larger the weight is, the more likely S_j will attract gaze. Normalizing the weights of all regions generates a probability map that represents the fixation pattern over the regions, integrated across all possible scan-paths.

2.2. SIGN Architecture

We develop the SIGN deep learning architecture to estimate the complex fixation duration (μ_0 and μ) and weight functions (w_j) in equations 2 and 3. Appendix 1 contains a diagram of the model’s architecture.

Modeling the Fixation Duration Functions μ_0 and μ . We use CNNs [14] to extract visual features, and use Multi-Layer Perceptrons (MLPs) to model the fixation-duration functions in relation to the image features. Particularly, μ_0 is produced by a MLP taking features S_0 and S_c from fine-tuneable ResNet50 models [8] on blurred \tilde{I} , respectively I^c , and μ is another MLP taking local features S_j from a simple fresh 5-layer CNN, whose inputs are raw image patches (regions).

Modeling the Weights w_j . The weights in equation 3 are a function of all local features S_j . The Transformer [26] is a natural candidate for the spatial modeling of those weights, as it integrates all visual features on the image. The Transformer takes in local features S_j from a simple 5-layer CNN. A MLP is then applied to learn a single weight for each transformed feature. A sigmoid activation is applied to the MLP output to ensure $w_j \in (0, 1)$ (see equation 2). Hence, the weights are modeled as:

$$w_j = \sigma(\text{MLP}(\text{Trf}([S_1, \dots, S_N]_j))), \quad (5)$$

where $\text{Trf}(\cdot)$ is the Transformer, S_j is the j th local feature vector, $\text{Trf}(\cdot)_j$ denotes the j th “transformed” local feature vector, and $\sigma(\cdot)$ is the sigmoid activation.

Context Effects If context I^c is present we include its effects in μ_0 (see the foundational model). The same fine-tuneable ResNet50 model used for the image extracts the visual features S_c from a down-scaled and blurred I^c , which are then concatenated with S_0 , those of the blurred image I , and fed into a MLP which produces μ_0 from the concatenated feature vectors.

3. Preliminary Results

We apply SIGN to two datasets, and compare its results with several benchmarks, in terms of accuracy of gaze prediction.

3.1. Data

AdGaze3500 [28] is a commercial dataset that contains 3531 digital display advertisements from the Dutch market. These ads come from 71 categories and appeared in 29 different mainstream digital magazines. Each ad image is either double-page or single-page accompanied by a counterpage (the context). Participants were asked to read the magazines freely as they would in their daily life. For each ad aggregate gaze data is available, collected by eye tracking of around 80-100 regular customers. Individual-level fixation locations are not available, making the training of SIGN more challenging.

COCO-Search18 [5] is a large-scale dataset that involves eye movements of “Target Absent” (TA) search tasks on 2489 images. Each image was shown to 10 participants and their eye fixations were recorded. Because we are interested in assessing the effectiveness of SIGN to recover personalized fixation patterns, our experiments use the gaze time data from the TA task of all images for only the first participant. We focus on the data of one individual to compare SIGN’s predicted weight maps with that individual’s observed fixations, but because the data is sparse we do not expect SIGN to be highly accurate in many cases and the results are reported here as an illustration only.

3.2. Training Procedure and Hyperparameters

Both datasets are randomly split into 90% for training and 10% for testing. 10-fold cross-validation is applied to the training data for an ensemble of 10 models. Images in the AdGaze3500 dataset were resized to 256×256 (height by width), and those in COCO-Search18 were resized to 256×416 . We use vanilla ResNet and Transformer models. The CNNs used to model local features S_j have 1 layer of 5×5 and 4 layers of 3×3 convolutions. We trained the free parameters of SIGN with respect to Mean Square Error (MSE) loss between the model predictions and the ground-truth; the parameters of its ResNet50 and Transformer modules are fine-tuned; all model parameters are trained simultaneously. For COCO-Search18, because the fixations are sparse we add a weak sparsity constraint on the weights in equation 3 as prior knowledge. The model is optimized by Adam optimizer [10]. We start the optimization with learning rates $1e-3$ and $1e-4$ for the AdGaze3500 and COCO-Search18 datasets respectively. We half the learning rate every 5 epochs with 60 epochs in total. We patchify the images as was done in [7] to obtain the spatial regions.

3.3. Patch Size Affects SIGN Performance

We test patch sizes of 8×8 , 16×16 , and 32×32 pixels on the AdGaze3500 dataset to evaluate their impact on prediction performance. We hypothesize that an optimal patch size exists that maximizes predictive accuracy: small regions may distort high-level semantic information, while large regions may miss fine-grained local details. Test-data loss (8×8 : 0.137, 16×16 : 0.134, and 32×32 : 0.135) reveals that a patch size of 16×16 is the optimal choice. An ablation experiment with AdGaze3500 shows that the gist of the context substantially reduces test-data loss (0.134 vs. 0.179).

3.4. SIGN Presents Better Gaze Predictions

We compare the performance of the proposed SIGN model with state-of-the-art baselines, including ResNet50 and ResNet101 [8], a Vision Transformer (ViT) [7], and a DeepGaze Saliency-based [13] MLP fine-tuned on each

dataset. We use test-data MSE and the correlation between the model predictions and the ground truth as performance measures. Table 1 presents the results. We observe that the proposed SIGN model outperforms all baselines on both datasets and on both measures. First, the improvement obtained by adding in SIGN a local gaze module to the ResNet50 model clearly indicates SIGN’s ability to extract more fine-grained local information that facilitates gaze prediction. Such an improvement is not simply obtained by introducing more parameters, because SIGN outperforms ResNet101 even though it uses fewer parameters ($\sim 37M$) than ResNet101 ($\sim 43M$). Apparently it is the architecture of SIGN rooted in our foundational model that produces improved prediction accuracy. Further we find that compared with the ViT, with a powerful spatial attention mechanism, ($\sim 87M$) parameters, and like SIGN 16×16 local image patches, SIGN achieves much higher predictive accuracy. Finally, comparing SIGN with DeepGaze shows SIGN’s contribution over a state-of-the-art saliency model. This shows that SIGN more efficiently exploits local features than a wide range of established models.

	AdGaze3500		COCO-Search18	
	MSE ↓	Corr. ↑	MSE ↓	Corr. ↑
ResNet50	0.141	0.81	0.216	0.61
ResNet101	0.138	0.82	0.221	0.60
ViT	0.194	0.63	0.218	0.60
DeepGaze+MLP	0.192	0.68	0.232	0.50
SIGN	0.134	0.83	0.212	0.62

Table 1. Comparing prediction accuracy across different models with MSE loss and correlation (Corr.) on the test data of the two datasets. Each result is the average of all 10 models from the 10-fold cross-validation.

3.5. SIGN Delivers Plausible Inferred Gaze Patterns

We normalized the trained weights in Equation 4 and plotted the resulting probability maps for the test images. Figures 1 and 2 show a few (non cherry-picked) samples; Appendix 2a and 2b contain additional samples. It is clear that the predicted maps trained on the AdGaze3500 data accurately capture headlines, products, and text blocks, which are regarded as the key design-regions of ads that attract gaze [22]. Due to the unstructured nature of the images from the COCO-Search18 data, the gaze pattern inferred from the probability maps is less well explainable. Nonetheless, for this individual’s data the predicted map overlaps with the observed fixations to a large extent, illustrating that the inferred map is plausible, probabilistically.

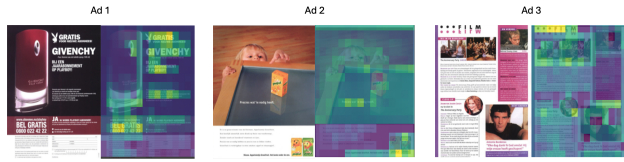


Figure 1. Sample predicted weight maps for AdGaze3500. For each sample, the left half presents the original image, and the right half presents the image overlaid with the generated SIGN weights. Brighter regions are predicted to be more conspicuous.

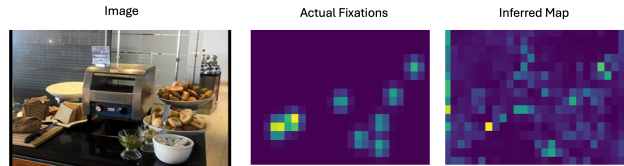


Figure 2. Sample predicted weight map for COCO-Search18 data. The original image is on the left, the actual fixation locations in the middle (blurred by a Gaussian filter with a standard deviation of 35 pixels [1] and resized), and the predicted inferred map is on the right.

4. Conclusion and Future Work

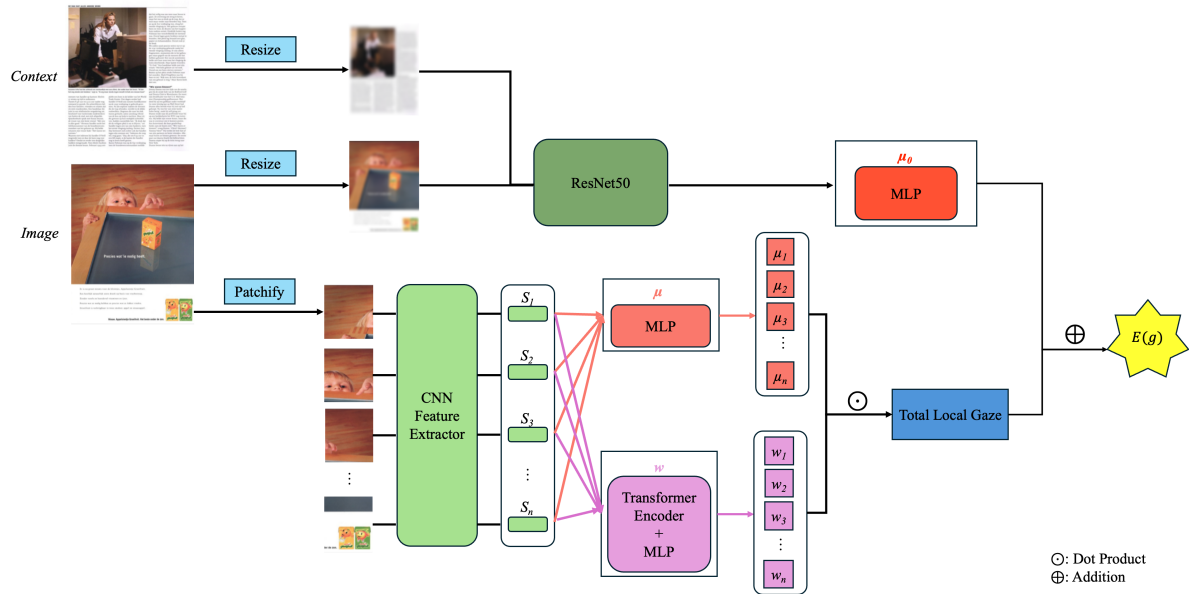
SIGN, our neural network model implementation of a foundational statistical formulation rooted in theories of attention and eye movements, shows promise in (1) predicting gaze time on images, and (2) generating plausible gaze patterns even when no individual fixation data are available.

While the initial results show that the generated gaze patterns correspond with observed ones, even when the model is trained on only aggregate gaze data, the accuracy of the SIGN-generated gaze patterns needs to be verified more extensively. Currently, it is not yet clear if SIGN generates accurate individual-level gaze maps for all individual search tasks in the COCO-Search18 data. The reasons are that first, the gaze pattern for individual-level search tasks are extremely sparse, and second that the images in this dataset have very heterogeneous spatial structures which makes it difficult for SIGN to generalize. Finally, currently SIGN is restricted to equally sized spatial regions, while people tend to look at regions that are semantically coherent and irregular hypothesize that SIGN may perform better for regions that contain coherent semantic information.

Overall, these initial findings provide valuable insights into SIGN’s strengths and areas that may require further optimization through subsequent experimentation and model refinement. In addition, SIGN can be used as a reward model to improve gaze on advertisements, with the ultimate goal of better matching advertised products and services to consumers’ needs, and thus have a positive societal impact.

References

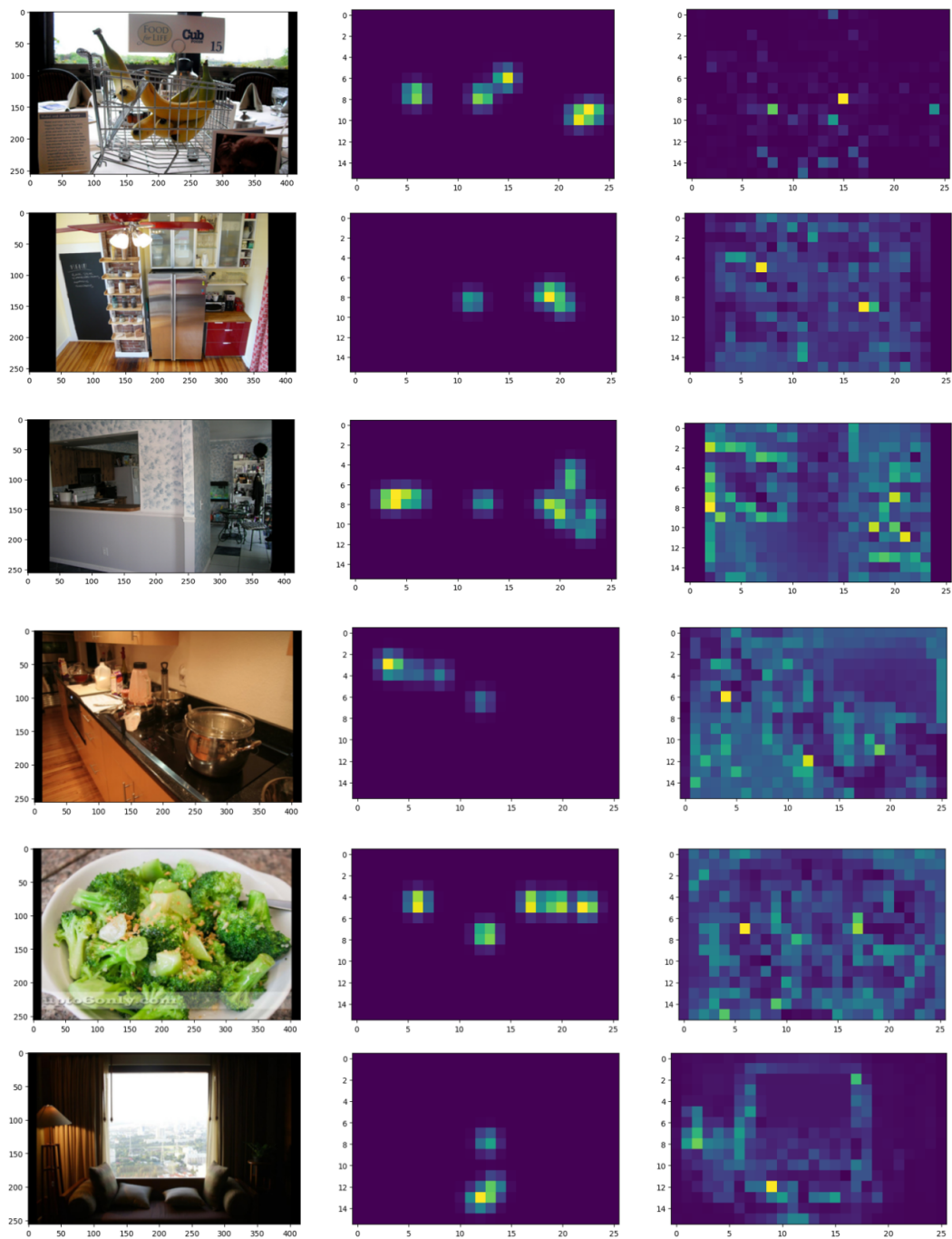
- [1] Zoya Bylinskii, Tilke Judd, Aude Oliva, Antonio Torralba, and Frédo Durand. What do different evaluation metrics tell us about saliency models? *IEEE transactions on pattern analysis and machine intelligence*, 41(3):740–757, 2018. 4
- [2] Sean Anthony Byrne, Adam Peter Frederick Reynolds, Carolina Biliotti, Falco J Bargagli-Stoffi, Luca Polonio, and Massimo Riccaboni. Predicting choice behaviour in economic games using gaze data encoded as scanpath images. *Scientific Reports*, 13(1):4722, 2023. 1
- [3] Xianyu Chen, Ming Jiang, and Qi Zhao. Predicting human scanpaths in visual question answering. In *Proceedings of the IEEE/CVF Conference on Computer Vision and Pattern Recognition*, pages 10876–10885, 2021. 1
- [4] Xianyu Chen, Ming Jiang, and Qi Zhao. Gazexplain: Learning to predict natural language explanations of visual scanpaths. In *European Conference on Computer Vision*, pages 314–333. Springer, 2025. 1
- [5] Yupei Chen, Zhibo Yang, Seoyoung Ahn, Dimitris Samaras, Minh Hoai, and Gregory Zelinsky. Coco-search18 fixation dataset for predicting goal-directed attention control. *Scientific reports*, 11(1):1–11, 2021. 1, 3
- [6] Marcella Cornia, Lorenzo Baraldi, Giuseppe Serra, and Rita Cucchiara. Predicting human eye fixations via an lstm-based saliency attentive model. *IEEE Transactions on Image Processing*, 27(10):5142–5154, 2018. 1
- [7] Alexey Dosovitskiy. An image is worth 16x16 words: Transformers for image recognition at scale. *arXiv preprint arXiv:2010.11929*, 2020. 3
- [8] Kaiming He, Xiangyu Zhang, Shaoqing Ren, and Jian Sun. Deep residual learning for image recognition. In *Proceedings of the IEEE conference on computer vision and pattern recognition*, pages 770–778, 2016. 3
- [9] Laurent Itti, Christof Koch, and Ernst Niebur. A model of saliency-based visual attention for rapid scene analysis. *IEEE Transactions on pattern analysis and machine intelligence*, 20(11):1254–1259, 1998. 1
- [10] Diederik P Kingma. Adam: A method for stochastic optimization. *arXiv preprint arXiv:1412.6980*, 2014. 3
- [11] Raymond M Klein. Inhibition of return. *Trends in cognitive sciences*, 4(4):138–147, 2000. 2
- [12] Matthias Kümmerer, Matthias Bethge, and Thomas SA Wallis. Deepgaze iii: Modeling free-viewing human scanpaths with deep learning. *Journal of Vision*, 22(5):7–7, 2022. 1
- [13] Matthias Kümmerer, Lucas Theis, and Matthias Bethge. Deep gaze i: Boosting saliency prediction with feature maps trained on imagenet. *arXiv preprint arXiv:1411.1045*, 2014. 1, 3
- [14] Yann LeCun, Léon Bottou, Yoshua Bengio, and Patrick Haffner. Gradient-based learning applied to document recognition. *Proceedings of the IEEE*, 86(11):2278–2324, 1998. 3
- [15] Seungho Lee, Minhyun Lee, Jongwuk Lee, and Hyunjung Shim. Railroad is not a train: Saliency as pseudo-pixel supervision for weakly supervised semantic segmentation. In *Proceedings of the IEEE/CVF conference on computer vision and pattern recognition*, pages 5495–5505, 2021. 1
- [16] John Liechty, Rik Pieters, and Michel Wedel. Global and local covert visual attention: Evidence from a bayesian hidden markov model. *Psychometrika*, 68:519–541, 2003. 1
- [17] Nian Liu and Junwei Han. Dhsnet: Deep hierarchical saliency network for salient object detection. In *Proceedings of the IEEE conference on computer vision and pattern recognition*, pages 678–686, 2016. 1
- [18] Sounak Mondal, Zhibo Yang, Seoyoung Ahn, Dimitris Samaras, Gregory Zelinsky, and Minh Hoai. Gazeformer: Scalable, effective and fast prediction of goal-directed human attention. In *Proceedings of the IEEE/CVF Conference on Computer Vision and Pattern Recognition*, pages 1441–1450, 2023. 1
- [19] David Noton and Lawrence Stark. Scanpaths in saccadic eye movements while viewing and recognizing patterns. *Vision research*, 11(9):929–IN8, 1971. 1
- [20] Antje Nuthmann. Fixation durations in scene viewing: Modeling the effects of local image features, oculomotor parameters, and task. *Psychonomic bulletin & review*, 24(2):370–392, 2017. 2
- [21] Aude Oliva and Antonio Torralba. Building the gist of a scene: The role of global image features in recognition. *Progress in brain research*, 155:23–36, 2006. 2
- [22] Rik Pieters and Michel Wedel. Attention capture and transfer in advertising: Brand, pictorial, and text-size effects. *Journal of marketing*, 68(2):36–50, 2004. 1, 4
- [23] Savannah Wei Shi, Michel Wedel, and FGM Pieters. Information acquisition during online decision making: A model-based exploration using eye-tracking data. *Management Science*, 59(5):1009–1026, 2013. 1
- [24] Benjamin W Tatler. The central fixation bias in scene viewing: Selecting an optimal viewing position independently of motor biases and image feature distributions. *Journal of vision*, 7(14):4–4, 2007. 2
- [25] Moshe Unger, Michel Wedel, and Alexander Tuzhilin. Predicting consumer choice from raw eye-movement data using the retina deep learning architecture. *Data Mining and Knowledge Discovery*, 38(3):1069–1100, 2024. 1
- [26] Ashish Vaswani, Noam Shazeer, Niki Parmar, Jakob Uszkoreit, Llion Jones, Aidan N Gomez, Łukasz Kaiser, and Illia Polosukhin. Attention is all you need. *Advances in Neural Information Processing Systems*, 30, 2017. 3
- [27] Wenguan Wang, Jianbing Shen, Xingping Dong, and Ali Borji. Salient object detection driven by fixation prediction. In *Proceedings of the IEEE conference on computer vision and pattern recognition*, pages 1711–1720, 2018. 1
- [28] Jianping Ye, Michel Wedel, and FGM Pieters. Contextual advertising with theory-informed machine learning. *Available at SSRN 5007216*, 2024. 1, 3
- [29] Yu Zeng, Yunzhi Zhuge, Huchuan Lu, and Lihe Zhang. Joint learning of saliency detection and weakly supervised semantic segmentation. In *Proceedings of the IEEE/CVF international conference on computer vision*, pages 7223–7233, 2019.
- [30] Jie Zhang, Michel Wedel, and Rik Pieters. Sales effects of attention to feature advertisements: A bayesian mediation analysis. *Journal of marketing research*, 46(5):669–681, 2009. 1



Appendix 1: Diagram of SIGN Architecture. The architecture consists of two separate parts, respectively corresponding to image and context ‘gist’ μ_0 and total gaze on image regions defined in equation 2. The “gist” is represented by the global visual features extracted by a pre-trained and fine-tunable ResNet50 block, which are then passed to μ_0 , modeled by an MLP, to calculate the gaze induced by the “gist”. In parallel, the original image is patchified into regions, which are subsequently compressed to local visual features S_1, S_2, \dots, S_n generated by a trainable CNN. Each local feature S_i is used to determine local gaze μ_i through an MLP; local features are also used to calculate local weights w_i , calculated from another MLP on top of a transformer encoder that enhances interactions among local features. The total local gaze pattern is calculated as the dot product between the local gaze and their local weights; the final predicted gaze is the sum of the “gist” gaze and the total local gaze pattern.



Appendix 2a: Additional Predicted Weight Maps for AdGaze3500.



Appendix 2b: Additional Predicted Weight Maps for COCO-Search 18.